

Structure and Microstructure Properties of Ball Milled Fe-Zn

R. Bensalem¹, O. Guergueb¹, S. Alleg¹, A. Younes¹, S. Souilah¹, M. Bououdina², J.J. Suñol³

¹ *Laboratoire de Magnétisme et Spectroscopie des Solides, Département de physique, Université de Annaba, B.P. 12 23000 Algérie*

² *Dep. of Physics, Bahrain University, Bahrain*

³ *Dep. de Física, universitat de Girona, Compus Montilivi, 17071, Girona Spain*

(Received 20 May 2013; published online 31 August 2013)

Nanocrystalline Fe₁₀ %Zn and Fe₃₀ %Zn alloys have been prepared from pure elemental powders by mechanical alloying processing in a high energy planetary ball-mill. Microstructural, structural, and magnetic characterizations of the powders were investigated by X-ray diffraction, and vibrating sample magnetometer. The crystallite size reduction to the nanometer scale is accompanied by an increase in the atomic level strain. The reaction between Fe and Zn leads to the formation of a bcc Fe(Zn) solid solution with a lattice parameter close to (0.2912 nm for Fe₃₀ %Zn and 0.2885 nm for Fe₁₀ %Zn) after 5 h of milling. The complete dissolution of the elemental Zn powders in the α -Fe lattice gives rise to the formation of a highly disordered Fe(Zn) solid solution, where α -Fe(Zn) nanograins have a crystallite size of (229,29 Å for Fe₁₀ %Zn (24 h) 30,09 Å for Fe₃₀ %Zn (24 h), on prolonged milling time. The coercivity and magnetization values are 18,90 (Fe₁₀ %Zn)Oe and 26,59 (Fe₃₀ %Zn) emu/g, respectively, after 24 h of milling.

Keywords: Nanocrystalline alloys, Mechanical alloying, X-ray diffraction, Scanning electron microscopy, Vibrating sample magnetometer.

PACS numbers: 75.60.Ej, 75.75.+a

1. INTRODUCTION

Fe-Zn alloys are used in the automotive industry as coating in order to prevent steel sheets from corrosion. The quality of the coating has been established to be directly related to the distribution of zinc atoms contained in it, so that the greater its distribution, the better the corrosion protection capability. However, given the significantly different melting temperatures of the metals (15351 °C for Fe and 4201 °C for Zn), synthesis of these alloys by conventional techniques, such as fusion, is not straightforward. Therefore, mechanical alloying (MA) appears as a feasible alternative for production of the powder with the desired microstructure. Therefore, the investigation of the Fe-Zn system by MA is of great relevance as far as technological importance is concerned, and also because it represents an excellent model system for establishing the relationships between macroscopic and microscopic processes and their evolution in time, given that it is not chemically inert and forms solid solutions. It allows, for example, relating microstructural features, such as crystallite size, lattice parameter and microhardness, to the processes that occur at a macroscopic scale. Investigating these relationships is the aim of the present work. MA is a powerful technique in the production of non-equilibrium / special metallic alloys, including solid solution systems and their extension from equilibrium limits (amorphous, nanocrystalline, quasicrystalline and supersaturated solid solution) [1-3]. Due to the large density of dislocations introduced by heavy plastic deformation during the milling process, a significant increase in solubility has been reported in many systems [4, 5]. Nanomaterials present a variety of superior properties than conventional materials due to their unique structure. The structure of nanocrystalline materials is characterized by a significant volume fraction of grain boundary regions and hence their behavior is

expected to have a strong influence on the properties of the materials [6, 7]. However, for large-scale applications, important macroscale properties of the mechanically alloyed powders must be attained in regard to on powder metallurgy processes, given the direct correlation with energy consumption during milling. Among these, the particle size distribution and morphology can be cited.

Relationships between chemical composition, evolution of the morphology and the microstructural stage of the powder particles have not been investigated in enough detail and in a systematic way in the literature, at least for systems capable of solid solution formation. Descriptions of the evolution of extended solid solutions by the MA process and its energetic correlation are not yet well established. In fact, little is known of the relationships between macroscopic (particle agglomeration, fracture, folding, etc.) and microscopic (reduction in crystallite size, solid solution extension, amorphization, phase transformation, etc.) processes that occur during MA. The detailed understanding of the phenomenology of these relationships is useful in developing effective mathematical models of MA. Nanostructured Fe-based magnetic materials have received considerable attention not only because of their unusual mechanical and magnetic properties which stem from the refinement of the crystallite size to the nanometer scale and from the enhanced density of defects [8-11], but also they are promising candidates for wide applications in technology such as, coating against corrosion, power transformers, inductors, components for data communication interface [12-14].

The present work attempts to study the formation mechanism of nanostructured Fe-Zn alloys prepared from elemental Fe and Zn pure powders. X-ray diffraction (XRD), scanning electron microscopy (SEM), and vibrating sample magnetometer (VSM) were used to analyze the changes in structural, microstructural and magnetic properties of this compound.

2. EXPERIMENTAL PROCEDURE

The alloyed nanostructured Fe10%Zn and Fe30%Zn alloys were prepared by a so-called Retsch PM400 planetary high energy ball mill starting from a mixture of Fe and Zn powders. Pure elemental powders of Fe (99.9% < 10 μm), Zn (99.9% < 45 μm), were mixed to give a nominal composition of Fe10%Zn and Fe30%Zn (atm %). The milling process was performed at room temperature under argon atmosphere using hardened steel vials and balls (5 balls with a diameter of 12 mm). The ball-to-powder weight ratio was about 2 : 1. The rotation speed was about 350 rpm. The milling process was interrupted each hour for half an hour in order to avoid the local temperature rise inside the vials.

Morphological changes of the powder particle during the milling process were followed by scanning electron microscopy (SEM) in DSM960A Zeiss equipment.

The magnetic measurements were performed in a vibrating sample magnetometer (VSM) at 300 K in an external field up to 10 kOe.

Structural and microstructural evolution in the milled powders were investigated by X-Ray diffraction (XRD) measurements on Bruker D8 advance diffractometer in a $(\theta - 2\theta)$ geometry using Cu-K α radiation ($\lambda = 0.154056$ nm). The structural and microstructural parameters were obtained from the Rietveld refinement of the XRD patterns by using the MAUD program [19].

3. RESULTS AND DISCUSSION

3.1 Structural and Microstructural Properties

Fig. 1 and Fig. 2 show the X-ray diffraction patterns of the starting and as-milled Fe10%Zn and Fe30%Zn powders, respectively, for various milling times. The top curve shows the X-ray diffraction pattern of a mixture of pure crystalline Fe and Zn peaks. It can be seen that as milling time increases, the intensity of the peaks decrease and the peaks become broader indicating the decrease in grain size down to the nanometer scale and an increase in microstrain.

The XRD pattern of the raw mixture (0 h) displays the Bragg diffraction peaks of the α -Fe, and Zn. Initial crystalline structure of reactants and products are: α -Fe with lattice parameter $a_0 = 0.2866$ nm and a space group Im3m, Zn with lattice parameter $a_0 = 0.3614$ nm and space group Fm-3m. The Bragg diffraction peaks of elemental bcc Fe, and Zn are still observed after of milling. The reaction between Fe and Zn, in the early stage of milling, can be related to the negative enthalpy of mixing (-39 KJ/mol) [20]. Ball milling of these elements leads to the splitting of Fe peaks and the formation of Fe(Zn) solid solution. After 24 h of milling, it is observed a complete disappearance of Zn peaks. Accordingly, the best Rietveld refinement has been performed and the results are shown in Fig. 3 and 4 for both solid solutions. This indicates that most of the elements have dissolved into the α -Fe lattice except for the mixture Fe(30)Zn where an excess of Fe is present. The formation, at room temperature of these solid solutions which are thermodynamically stable

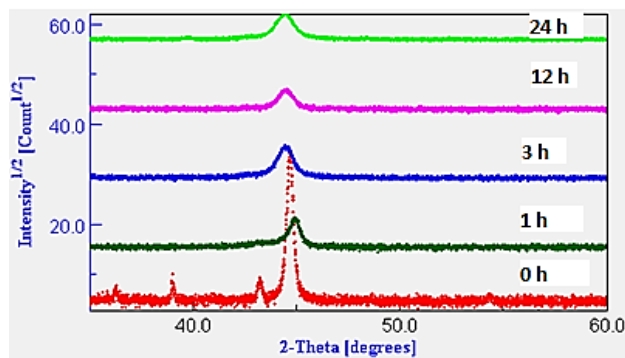


Fig. 1 – XRD-ray diffraction patterns of Fe-10%Zn for different milling times

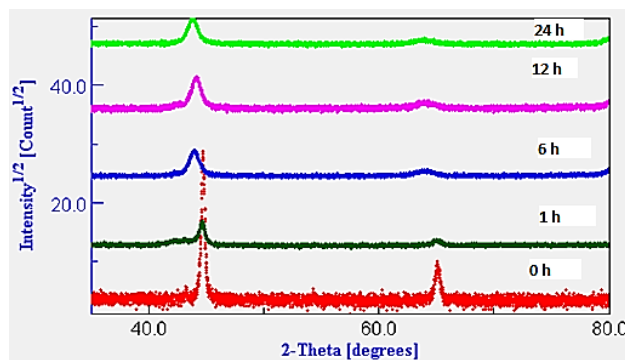


Fig. 2 – XRD-ray diffraction patterns of Fe-30%Zn for different milling times

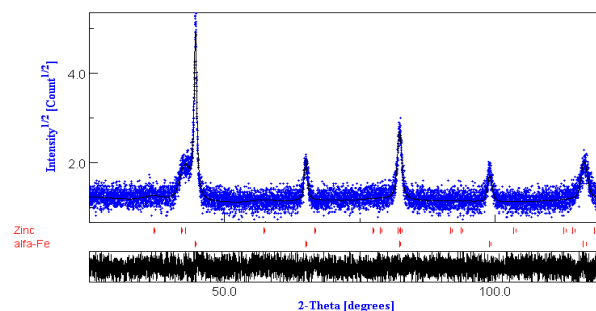


Fig. 3 – Best Rietveld refinement of XRD-ray diffraction patterns of Fe-30%Zn

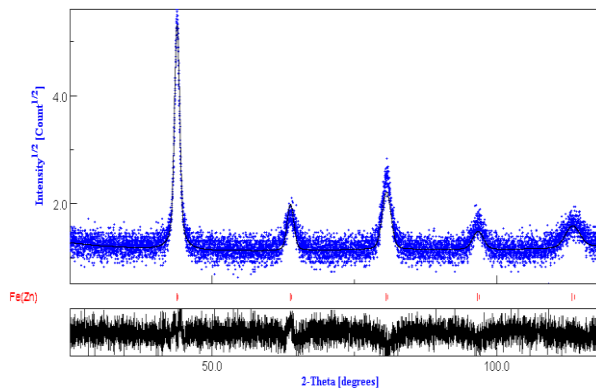


Fig. 4 – Best Rietveld refinement XRD-ray diffraction patterns of Fe-30%Zn

can be assigned to the crystallite size refinement and to

the induced structural defects $\langle \sigma^2 \rangle^{1/2}$.

The obtained product on prolonged milling time consists of a highly disordered Fe(Zn)-type solid solution.

The evolution of the different microstructure parameters such as lattice parameters, average crystallite sizes $\langle L \rangle$, phase volume percentages (%) and microstrains $\langle \sigma^2 \rangle^{1/2}$, as a function of milling time are presented in figures 5-7, for the phase obtained by Rietveld refinement. One observe that the lattice parameter decreases in general when milling time increases from 4 h to 24 h. The decrease of the lattice parameter in the first stage can be due to the progressive dissolution of small Zn atoms into the α -Fe lattice. This behavior of the lattice parameter has to be attributed to the structural distortions induced by the progressive diffusion of Zn into the α -Fe lattice. Indeed, it is well known that the substitutional solutes can either dilate or contract the host lattice depending on the relative atomic sizes of these elements with respect to the solvent atom.

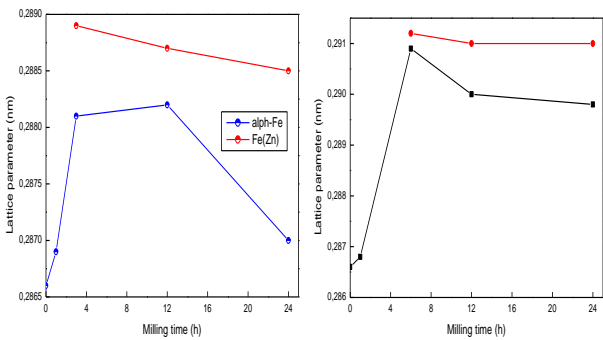


Fig. 5 – Lattice parameter evolution of α -Fe and Fe (Zn) solid solution of the Fe-10 %Zn and Fe-30 %Zn powders vs milling time

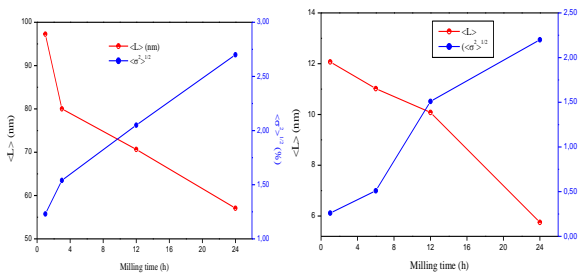


Fig. 6 – Crystallite sizes and lattice microstrain of Zn for Fe-10 %Zn versus milling time

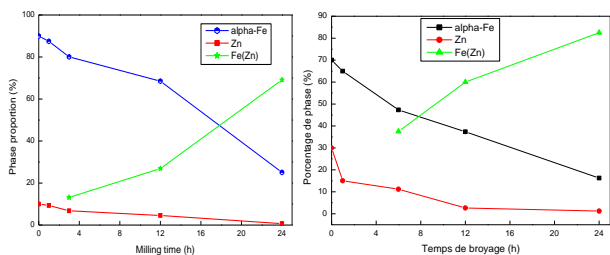


Fig. 7 – Percentage volume phases of Zn, α -Fe, Fe(Zn) solid solution, as a function of milling time of Fe-10 %Zn and Fe-30 %Zn, respectively

The relative deviation of the lattice parameter from that of the perfect crystal, which is defined by $\Delta a = \frac{a - a_0}{a_0}$ reaches, as much as $\Delta a = 0.017\%$. This re-

flects the effect of the plastic deformation and the introduction of several defects into the host F lattice during the milling process. This deviation is smaller than that reported for the milled pure Fe ($\Delta a = 0.28\%$) [24]. Such a difference might be linked to the milling conditions.

Because of deformation and fracturing of the powder particles, grains may be refined as shown in Fig. 6 which shows the average crystallite size, $\langle L \rangle$, and the root-mean square strain, $\langle \sigma^2 \rangle^{1/2}$ of Fe as a function of milling time. The crystallite size decreases during the milling down to the nanoscale, simultaneously the microstrains increase owing to the external deformation influence and the internal microdeformation. This is attributed to the fact that the small crystallite size provides itself a limit for the dislocation glide and consequently, for more crystallite size reduction.

3.2 Magnetic Measurement

Fig. 8 shows the milling dependence of the hysteresis loops, at 300 K, of the ball-milled Fe-10 %Zn and Fe-30 %Zn powders, respectively. The applied magnetic field varies from -1000 to 1000 Oe. These sigmoidal

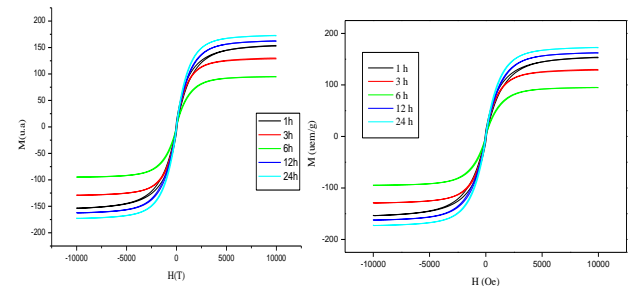


Fig. 8 – The milling dependence of the hysteresis loops, at 300 K, of the ball-milled Fe-10 %Zn and Fe-30 %Zn powders

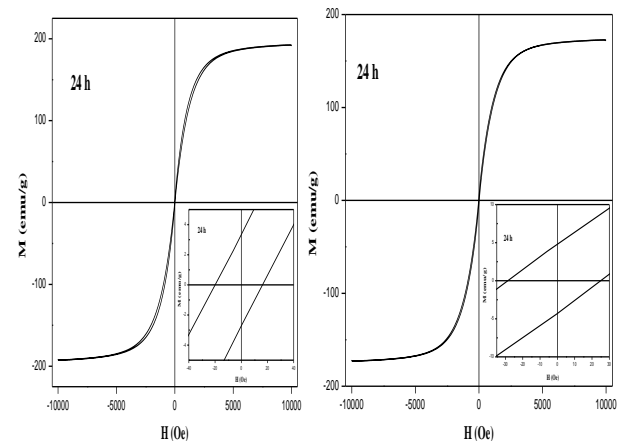


Fig. 9 – The Hysteresis loops, at 300 K, of the ball-milled Fe-10 %Zn and Fe-30 %Zn powders after 24 h of milling

hysteresis cycles are usually observed in nanostructured samples with small magnetic domains. The small hysteresis losses are properties generally desired in soft magnetic materials [25, 26]. This is due not only to the presence of structural distortions inside

grains, but also to a higher density of precipitates which hinder the domain wall movement. In the case of Fe-30%Zn H_c increases from 15 Oe before milling to 45 Oe after 24 h of milling, and then should remain nearly constant on further milling [22]. The difference may be ascribed to the presence of Zn.

Fig. 9 illustrates the hysteresis cycle for both mixture Fe-10%Zn and Fe-30%Zn powders, respectively, ball-milled for 24 h. The insert showing a magnification around the origin of the cycle proves the anisotropic magnetic behavior of the materials.

REFERENCES

1. C.C. Koch, *Ann. Rev. Mater. Sci.* **19**, 121 (1989).
2. H. Zoz, *Mater. Sci.* **19**, 121 (1989).
3. D. Basset, *P. Mater. Sci. Eng.* **168**, 149 (1993).
4. C. Bansal, Z.Q. Gao, L.B. Hong, B. Fultz, *J. Appl. Phys.* **76**, 5961 (1994).
5. C.C. Koch, *Nanostruct. Mater.* **2**, 109 (1993).
6. R.B. Schwarz, C.C. Koch, *Appl. Phys. Lett.* **49**, 449 (1986).
7. S.U. Kim, K.H. Kim, Y.M. Koo, *J. Alloy. Compd.* **368**, 357 (2004).
8. H. Gleiter, *Prog. Mater. Sci.* **33**, 223 (1989).
9. K.S. Kumar, H. Van Swygenhoven, S. Suresh, *Acta Mater.* **51**, 5743 (2003).
10. C.B. Jiang, M. Venkatesan, K. Gallagher, J.M.D. Coey, *J. Magn. Mater.* **236**, 49 (2001).
11. F.N. Frase, R.D. Shull, L.B. Hong, T.A. Stephens, Z.Q. Gao, B. Fultz, *Struc. Mater.* **11**, 987 (1999).
12. K. Suzuki, N. Kataoka, A. Inoue, A. Makino, T. Masumoto, *Mater. Trans. JIM* **31**, 743 (1990).
13. A. Makino, K. Suzuki, A. Inoue, T. Masumoto, *Mater. Trans. JIM* **32**, 551 (1991).
14. A. Makino, T. Hatanai, A. Inoue, T. Masumoto, *Mat. Sci. Eng. A* **226-228**, 594 (1997).
15. M. Müller, N. Mattern, L. Illgen, *J. Mag. Mag. Mater.* **112**, 263 (1992).
16. J.D. Ayers, V.G. Harris, J.A. Sprague, W.T.H.N. Elam, Jones, *Acta Mater.* **46** No 6, 1861 (1998).
17. S. Suriñach, M.D. Baró, J. Segura, M.T. Clavaguera-Mora, N. Clavaguera, *Mater. Sci. Eng. A* **134**, 1368 (1991).
18. H. Okumura, K.N. Ishihara, P.H. Shingu, H.S. Park, S. Nasu, *J. Mater. Sci.* **27**, 153 (1992).
19. L. Lutterotti, *MAUD CPD Newsletter (IUCr)* **24** (2000).
20. F.R. De Boer, R. Boom, W.C.M. Mattens, A.R. Miedema, A.K. Niesser, *Cohesion in Metals: Transition Metal Alloys, 217* (North Holland, Amsterdam: The Netherlands: 1989).
21. K. Iizumi, C. Sekiya, S. Okada, K. Kudou, T. Shishido, *J. Eur. Ceram. Soc.* **26**, 635 (2006).
22. S. Alleg, M. Ibrir, N.E. Feninecheb, S. Azzaza, R. Bensalem, J.J. Suñole, *J. Alloy. Compd.* **494**, 109 (2010).
23. S. Miraghaei, P. Abachi, H.R. Madaah-Hosseini, A. Bahrami, *J. Mater. Proc. Tech.* **203**, 554 (2008).
24. S. Azzaza, S. Alleg, H. Moumeni, A.R. Nemancha, J.L. Rehspringer, J.M. Grenech, *Condens. Mat.* **8**, 7257 (2006).
25. A.M. Berkowitz, E. Kneller, *Magn. and Metal.* **1** (Academic Press: New York: 1969).
26. W.F. Smith, *Principles of Materials Science and Engineering* (McGraw-Hill: New York: 1986).

4. CONCLUSION

X-ray diffraction, and vibrating sample magnetometer were used jointly to study the structural, microstructural and magnetic properties of the mechanically alloyed Fe-10%Zn and Fe-30%Zn powders. A mixture of Fe(Zn) type solid solution is obtained after 24 h of milling, where the crystallite size decreases to the nanometer scale.